RESEARCH

KEPCO Journal on Electric Power and Energy
p-ISSN 2465-8111, e-ISSN 2466-0124
Volume 7, Number 1, June 2021, pp. 125-128
DOI 10.18770/KEPCO.2021.07.01.125

Failure Analysis of Circulating Water Pump Shaft in Power Plant

발전 계획에서 순환 물 펌프 고장 분석

Jaehong Lee, Nam-gun Jung

Abstract

This paper presents the root cause failure analysis of the circulating water pump in the 560 MW thermal power plant. A fractured austenitic stainless-steel shaft operated for 24 years was examined. Fracture morphology was investigated by micro and macro-fractographic analysis. The metallurgical analyses including chemical analysis, metallography and hardness testing were performed. The analysis reveals that the pump shaft was fractured due to the reverse bending load with combination of rotating bending load. Corrective actions for plant operator was recommended based on the analysis.

Keywords: *Circulating Water Pump, Fractography, Fatigue, Reversed Bending, Stress Concentration*

I. Introduction

A circulating water pump is one of the critical equipment for the continuous operation of a power plant, providing water to and through the condenser for cooling. The vertical type pumps are normally used for the plant using the sea water for cooling exhaust steam due to its efficiency.

Fatigue is the most common failure mechanism of pump shafts. In order for fatigue to occur, a cyclic tensile stress is necessary as well as a crack initiation site in the form of a stress concentration. Thus, rotating elements on pumps such as shaft, are susceptible to fatigue by the nature of their operation [1]. Vertical pumps can exhibit high vibration levels than horizontal mounted pumps. These pumps often operate with signs of unstable operation, large misalignments, and other characteristics that would cause immediate shutdown in most power plant [2]. The most common problem that can be found in any pump assembly are shaft unbalance and misalignment. Disassembly and reassembly of long vertical pumps should be precisely done, as it requires more attention than horizontal pumps [3].

The circulating water pump had broken down in the 560 MW power plant after 24 years in-service. A 10-meter-length shaft of vertical pump was fractured at the location where 5 mm-depth split ring groove exists 4.4 meters down from the top shown in Fig. 1. The shaft was made of 316L stainless steel and has a diameter of 220 mm in the design.

In this paper, the failure of circulating water pump shaft was investigated to reveal loading history through fracture surface analysis. The metallurgical examination was also performed for clarification of the issues on the materials. Finally, some recommendations were provided to prevent possible accident with the issue in operation.

II. Experimental Procedure

The experimental investigation was executed in the following sequence:

1) Chemical analysis of the shaft by energy dispersive spectrometry;
2) Hardness measurement by a Rockwell B tester;
3) Metallographic examination of a cross section sample with respect to the longitudinal direction by an optical microscope;
4) Macro-fractography of the fracture surface by visual examination;
5) Micro-fractography of the fracture surface by means of an electron microscope.

III. Result and Discussion

A. Chemical Analysis

Chemical composition of the shaft was obtained by using the electron dispersive spectrometer onto the longitudinally sectioned sample on the central axis about 20 mm away from the fracture. The resultant chemical composition by its weight was corresponds to ASTM A276-316L stainless steel standard only except slightly higher chromium composition. Chromium plays role in enhancing

Article Information

Manuscript Received March 02, 2020, Revised June 19, 2020, Accepted September 10, 2020, Published online June 30, 2021

The Authors are with KEPCO Research Institute, Korea Electric Power Corporation, 105 Munji-ro Yuseong-gu, Daejeon 34056, Republic of Korea.

Correspondence Author: *Jaehong Lee* (*jaehong.lee9@kepco.co.kr*)

ORCID: *0000-0002-6398-5228* (*J. Lee*); *0000-0002-6781-7731* (*N. Jung*)

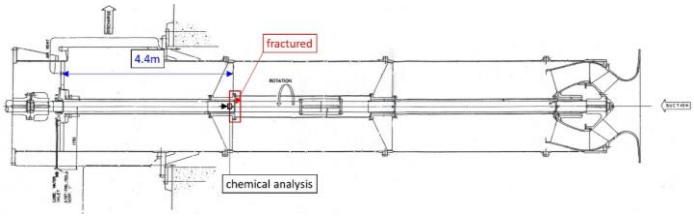

Fig. 1. A drawing of the failed circulating water pump. The fracture position in the shaft was indicated by red the arrow. The sectioning sample, which was examined in chemical analysis and microstructure and hardness in the next chapter, was indicated by the black square and its direction by the black arrow.

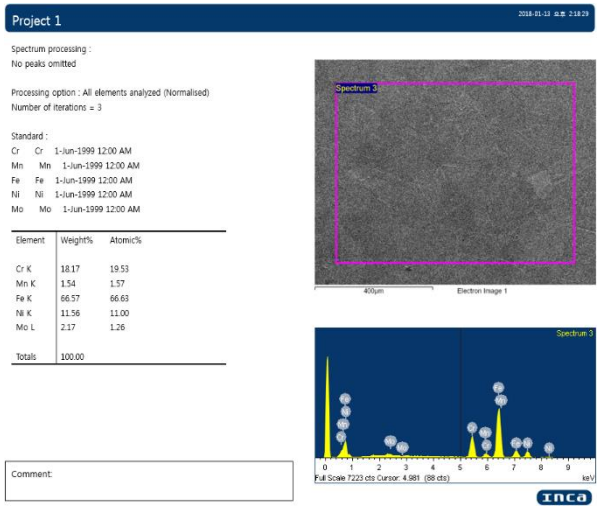

Fig. 2. Semi-quantitative EDX analysis of the shaft material

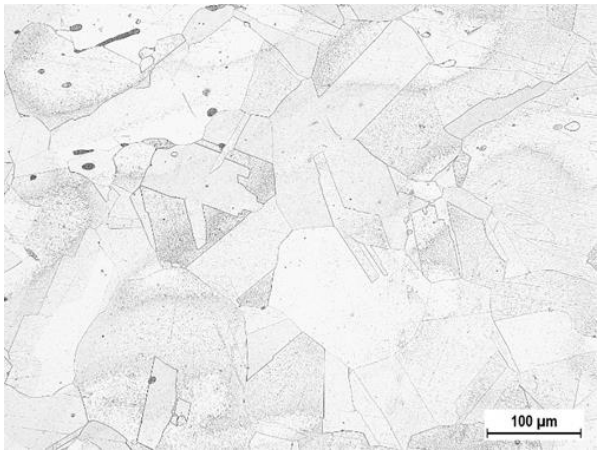

Fig. 3. Optical micrograph of the shaft. It shows no harmful microstructure such as heavy sensitization in low magnification.

corrosion resistance of the product made of steel alloy. No detrimental effect to the shaft failure due to the chromium composition was revealed in the following metallurgical analysis.

B. Microstructure and Hardness

The microstructure of the shaft sample was observed by using an optical microscope. The sample 20mm away from the fracture same as in chemical analysis was used. The surface of the specimen was etched by Vilella's reagent after being grinded by silicon carbide papers up to P800-grit and polished in sequential by 6 µm to 1 µm diamond as a slurry on cloths. Fig. 3 shows microstructure of the shaft made of austenitic stainless steel. Heavy sensitization effect such as wide and dark lines at the grain boundaries which can be easily shown even in low magnification micrograph was not found.

Rockwell B hardness testing was performed onto the sample. About 80 HRB was obtained which consistent with the ASTM A276-316L standard specification for manufacturing requirement, within maximum value of 95 HRB.

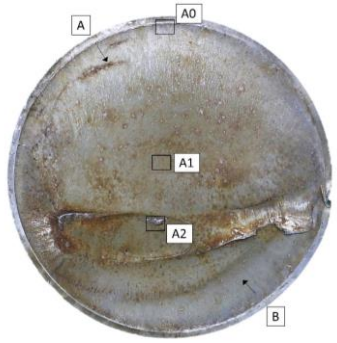

(a)

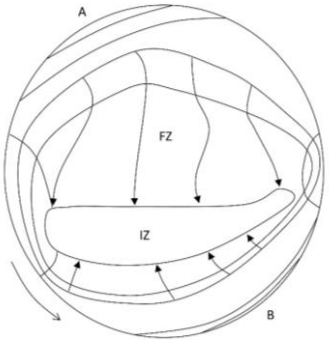

(b)

Fig. 4. Macro-fractography of the failed shaft. (a) The fracture surface of the failed shaft. Crack propagation direction was indicated by the arrow. (b) A schematic diagram of the fracture surface. Crack initiation site was named as 'A', 'B'. Fatigue zone and Instantaneous zone with expected fatigue propagation history were displayed in the figure.

TABLE 1
Chemical Composition of the Shaft Steel by EDX in SEM and ASTM A276-316L

Materials	C	Mn	P	S	Si	Cr	Ni	Mo	Fe
Shaft steel	-	1.54	-	-	-	18.17	11.56	2.17	bal.
ASTM A276-316L	0.030	2.00	0.045	0.030	1.00	16.0-18.0	10.0-14.0	2.00-4.00	bal.

C. Macro- and Micro-Fractography

Fig. 4 shows the fracture surface of the shaft obtained by digital camera and its schematic diagram of the fatigue crack progression

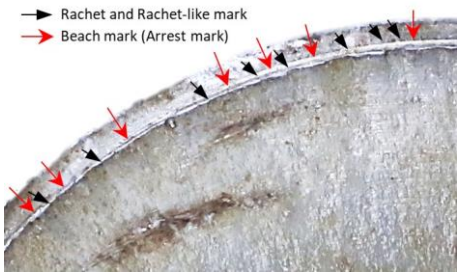

Fig. 5. Detailed fractography of the failed shaft. Oval beach marks, which is barely visible in the photograph, at the multiple points are indicated by the arrow. Rachet marks at the groove are also shown in the figure.

on the surface. The surface was chemically cleaned prior to fractographic inspection by organic and alkali solvents for elimination of debris, oil and rust to make the fracture surface features discernible such as ridges for striation. For applied load histories being well-preserved on the surface, no acidic cleaning solution was used [4]. First, it was treated by organic solvent cleaning and soft brush. Next, ultrasonic cleaning was performed in the ultrasonic bath with the alkaline detergent, ULTRAMET Sonic Cleaning Solution, provided by Buehler. A detailed photograph of the top left side in Fig. 4(a) is shown in Fig. 5. The rachet and rachet-like marks are revealed along the top left circumference of the shaft. It implies they were origin of the crack and high stress concentration or high stress had been applied to top-left region on the fracture surface. Multiple arrest marks colored in brown by oxidation also intensify the thesis. There is a similar zone where rachet-marks exists along the local circumstance of the shaft at the bottom and bottom-right on the surface in Fig. 4(a) but much milder than the top-left.

From the region a little below the top, there are numerous shiny ridges which travel downwards which implies unstable state of crack generation [5]. Afterwards, the surface becomes flatter while on the left side of the surface the clear shiny ridges exist. The flat surface changes dramatically to the hill-and-hole zone called the instantaneous zone (IZ) at the lower center of the surface which is usually generated due to the overload.

Using scanning electron microscope, the micro-fractography of 'A0', 'A1' and 'A2' in Fig. 4(a) was obtained. Fig. 6(a) shows the possible striations beneath the oxidized fracture surface in 'A0'. The fracture surface in this region was damaged attributed to post failure rubbing. In the region 'A1', striations are clearly visible which propagates to the bottom shown in Fig. 6(b). At instantaneous zone 'A2', there are numerous dimples which indicate ductile fractures shown in Fig. 6(c).

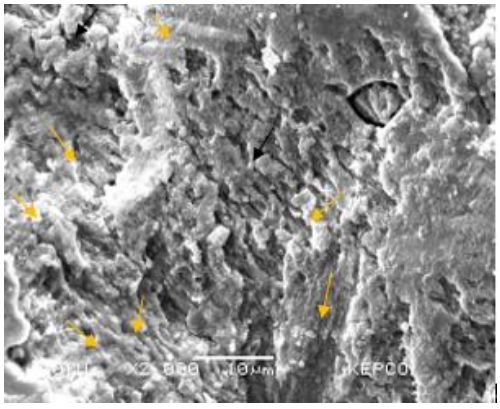

(a)

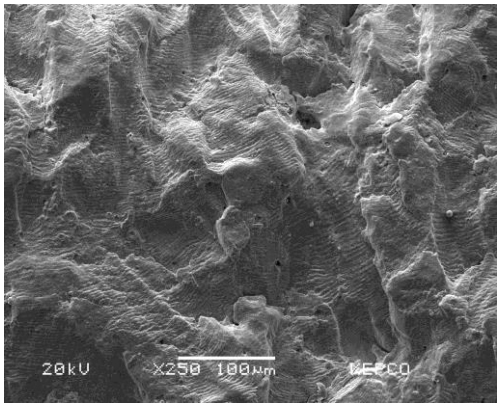

(b)

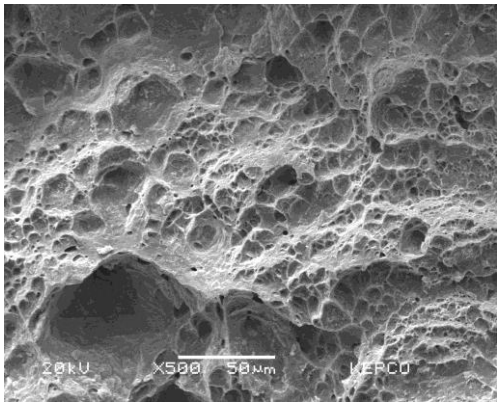

(c)

Fig. 6. Micro-fractography from scanning electron microscope (a) 'A0' in Fig. 3. Possible striations underneath the corroded surface indicated by the arrow. (b) 'A1' in Fig. 3. Patterns of striations revealed clearly. (c) 'A2' in Fig.3. Dimple patterns which exist on the surface.

D. Load Histories and Discussions

Fatigue crack forms at the location or the locations the local maximum stress has applied to and the minimum strength exists in [6]. Reversed bending occurs when the shaft flexes in two direction opposite to one another and two opposed points on the shaft experience maximum alternating tensile and compressive stress [1]. With consideration of the fatigue crack patterns on the fracture surface, we can trace back what kinds of loads applied and how much intense they were in the past. An area of the instantaneous zone (IZ), which is also called overload zone, is an indicative of final fracture load. Furthermore, its shape such as the roundness is an indication of types of applied loads. Also, the rachet marks and progression marks are the ones we can assume how much stress and stress concentration had influenced to the cracking. The fracture surface characteristics according to the type, local and global intensity of load are shown in Fig. 7 [6][7].

Fig. 4(b) shows a simplified schematic diagram of the fatigue fracture pattern of the failed shaft. Stress which had been applied to the shaft was low generally until final fracture occurred considering that small area of the IZ in Fig. 4(b). The oval shaped IZ can be considered as the result of a combination of the reversed bending

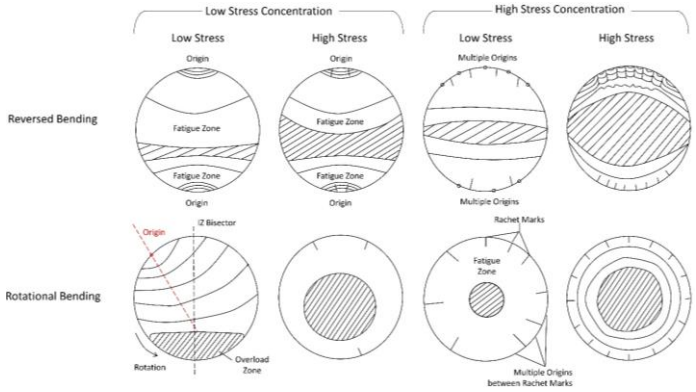

Fig. 7. Representative schematic diagrams of fatigue fracture according to types of load and stress concentration factor. The diagram was drawn by the author based on the combination of the knowledge in the literatures [6][7].

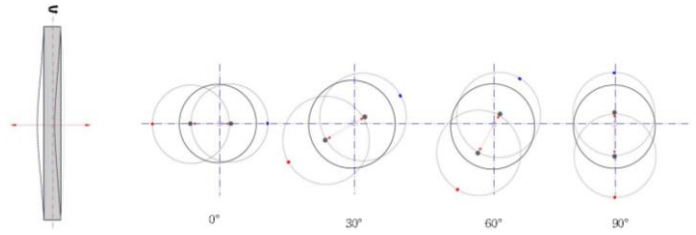

Fig. 8. Representative behavior of rotating shafts which induces reversed bending load.

and the rotating bending moment. Furthermore, its roundness is so small that the reversed bending was much more dominant than the rotating bending to the cracking. Rachet marks at the top as shown in Fig. 5(a) can make us confirms that there had been severe stress concentration, high stress or both on the shaft at the initial stage. The wide progression marks at the initial stage makes sense with the accordance to Fig. 7. At the propagation stage, stress had applied more intensely to the upper part than the lower part given the fact that progression marks at the upper fatigue zone are wider than the lower one.

In summary, at the initial stage, reversed bending moment with moderate to high stress and severe stress concentration had applied to the shaft. Afterwards, the crack had propagated subject to a combination of reversed bending and rotating bending with the intensity of low stress and high stress concentration.

In rotating shaft, reversed bending usually occurred by the shaft unbalance. Imbalance of the shaft make the eccentricity when a shaft rotates. This eccentricity makes bending deflections in the specific direction when the shaft rotating. The representative behavior of unbalanced shaft with the consideration of the load histories on the shaft are shown in Fig. 8.

Bearing misalignment also induce bending moment on a shaft but in the omni-directional way rotational bending which does not fit to reversed bending but to rotational bending.

High stress concentration at the location the diameter changes can be reduced by changing the roundness of the corner. Mechanical unbalance of shaft possibly results from by defects/errors in mechanical wear of impeller such as cavitation or erosion [8]. For the operator in the plant errors in assembly such as shaft alignment and runout examination should be managed thoroughly during an overhaul while manufacturing defects are inspected by the non-destructive testing. Wear of impeller can be easily noticed by pump maintenance workers during an overhaul. In operation, the presence of unbalance of the shaft can be primarily judged by high level of vibration. High vibration indication would be helpful stepping into subsequent inspection of the shaft during an overhaul, so that considerate vibration monitoring should be maintained.

IV. Conclusion and Recommendation

The failure analysis can be concluded as below:

1) The failure of circulating water pump shaft initiated and propagated by the fatigue;
2) The fatigue was derived from the reversed bending moment with a combination of rotating bending;
3) High stress concentration at the split ring groove was influenced to the fracture.

Recommendation for the preventive measure can be as following:

1) Shape improvement of split ring groove for less stress concentration was recommended;
2) Shaft alignment and runout examinations should be managed thoroughly;
3) Considerate vibration monitoring should be maintained after an overhaul.

References

[1] Berndt, F., A. Van Bennekom., "Pump shaft failures – a compendium of case studies," Engineering Failure Analysis, vol. 8, no. 2, pp. 135-144., 2001, https://doi.org/10.1016/S1350-6307(99)00043-6.

[2] Walter, T., Marchonie, M. M., Shugars, H. G., "Diagnosing Vibration Problems in Vertically Mounted Pumps," ASME. J. Vib., Acoust., Stress, and Reliab., Vol. 110, pp. 172-177, April, 1988, https://doi.org/10.1115/1.3269495.

[3] Abdel-Rahman, Sm. M., S. A. El-shaikh., "Diagnosis vibration problems of pumping stations: case studies," 13th IWTC (International Water Technology Conference) March, 2009, pp. 12-15.

[4] Mullen, Michael J., Arthur H. Griebel, John M. Tartaglia., "Fracture surface analysis," Advanced Materials and Processes, vol. 165, no. 12, pp. 21-23., 2007.

[5] Becker, W. T., Lampman, S., "Fracture appearance and mechanisms of deformation and fracture," Materials Park, OH: ASM International, 2002., pp. 559-586.

[6] Shipley, R. J., W. T. Becker. "ASM handbook," in Failure analysis and prevention, vol. 11. 10th ed., USA: ASM International, 2002. pp. 463.

[7] Sachs, N. W., "Understanding the surface features of fatigue fractures: how they describe the failure cause and the failure history," Journal of Failure Analysis and Prevention, vol. 5, no. 2, 2005, pp. 11-15. https://doi.org/10.1361/15477020522924.

[8] Bhave, Srikant. Mechanical Vibrations. Pearson Education India, 2010.